Journal of Catalysis 278 (2011) 153–161

Contents lists available at ScienceDirect

Journal of Catalysis

journal homepage: www.elsevier.com/locate/jcat

Correlation between deactivation and Pt-carbonyl formation during toluene hydrogenation using a H_2/CO_2 mixture

Aqeel Ahmad Taimoor [a], Isabelle Pitault [a,*], Frédéric C. Meunier [b,*]

[a] University of Lyon, CNRS, Laboratoire de Génie des Procédés Catalytiques, CPE Lyon, 43 bd du 11 novembre 1918, BP 82077, 69616 Villeurbanne Cedex, France
[b] Laboratoire Catalyse et Spectrochimie, University of Caen, CNRS, ENSICAEN, 6 Boulevard du Marechal Juin, 14050 Caen Cedex, France

ARTICLE INFO

Article history:
Received 15 October 2010
Revised 5 December 2010
Accepted 7 December 2010
Available online 8 January 2011

Keywords:
Biogas
CO_2
H_2
CO
Pt
Toluene
Hydrogenation
Reverse water–gas shift
Operando

ABSTRACT

H_2/CO_2 mixtures derived from biomass degradation may be regarded as a renewable source of hydrogen that could be used for hydrogenation reactions. The practicality of directly using a CO_2-containing H_2 feed was evaluated during the hydrogenation of toluene to methylcyclohexane at 75 °C and ambient pressure. An operando DRIFTS study was carried out to unravel some of the mechanistic features of this reaction over a 0.88% Pt/Al_2O_3 catalyst, in particular to rationalize the loss of activity observed in the presence of CO_2. We report, for the first time, a quantitative link between the loss of activity for hydrogenation and the formation of carbonyls adsorbed on the platinum, while the deactivation could not be correlated to the species formed onto the alumina, e.g. carbonates, hydrogenocarbonates and formates.

1. Introduction

Biogas produced by dark fermentation of organic wastes may consist of a mixture of mostly dihydrogen and carbon dioxide [1,2]. The possibility to directly use this mixture at low temperature and pressure as a renewable feedstock for hydrogenation reactions would be valuable. However, a possible difficulty associated with this feedstock is the potential reactivity of carbon dioxide. CO_2 is usually considered as an inert molecule, but it can lead, for instance, to carbon monoxide through the reverse water–gas shift reaction (RWGS, Eq. (1)) when an appropriate catalyst such as a Pt-group metal is present [3–5].

$$H_2 + CO_2 \rightarrow H_2O + CO \quad \Delta_r H^\circ(298\ K) = +42\ kJ/mol \tag{1}$$

The concentration of CO produced is small at low temperatures, first, because of thermodynamic limitations and second, because the reaction rates are minute below 250 °C for catalysts based on Pt [5–8]. However, even if the CO concentrations formed are low and possibly not detectable in the reactor effluent, CO traces may lead to a dramatic change of the activity of Pt-group metals, which are commonly used in hydrogenation reactions. The dissociative chemisorption energy of H_2 on the Pt(1 1 1) surface is typically comprised between 68 and 80 kJ/mol [9–11], while the CO binding energy on the same surface ranges from 144 to 173 kJ/mol [12,13]. Therefore, CO molecules bind more strongly to the Pt atoms than dissociating H atoms and may block the sites required for hydrogen adsorption and strongly decrease the hydrogenation rate. The poisoning effect will be worse if the molecule to be hydrogenated can only adsorb on the metal sites, hence be in competition with CO. Note that the adsorption enthalpy of toluene on Pt(1 1 1) is about 65 kJ/mol [14].

The poisoning of Pt catalysts by CO formed from CO_2 was actually reported by several authors. Baiker and co-workers showed by in situ IR spectroscopy that Pt, Ru, Rh and Pd were all gradually covered with carbonyl species under 90 bars of supercritical CO_2 ($scCO_2$) in the presence of 1% H_2 at 50 °C, with the Pt-based sample displaying the highest rate of carbonyl formation [15]. Baiker and co-workers [16,17] had reported earlier on the deactivation and low activity of a 5 wt.% Pt/Al_2O_3 in $scCO_2$ (80 bar of CO_2) at ca. 35 °C during ethyl pyruvate hydrogenation, which was ascribed to the reduction of CO_2 to CO, the latter species poisoning the metal surface. Xu et al. [18] have used a CO_2-containing medium for polystyrene ring hydrogenation and reported a deactivation due to CO formed from the RWGS (Eq. (1)) over a Pd-based catalyst at 150 °C,

---

* Corresponding authors.
E-mail addresses: isabelle.pitault@lgpc.cpe.fr (I. Pitault), frederic.meunier@ensicaen.fr (F.C. Meunier).

0021-9517/$ - see front matter © 2010 Elsevier Inc. All rights reserved.
doi:10.1016/j.jcat.2010.12.002

while the deactivation of a Ni-based catalyst (observed at 180 °C) was ascribed to water formed from the CO_2 methanation (Eq. (2))

$$4H_2 + CO_2 \rightarrow 2H_2O + CH_4 \quad \Delta_r H^\circ(298\ K) = -165\ kJ/mol \qquad (2)$$

The involvement of the RWGS was also noted in the case of the operation of low-temperature fuel cells. Van Zee and co-workers have shown that the reformate (i.e. CO_2, N_2 and H_2) used in a proton exchange membrane fuel cell (PEMFC) at 70 °C led to the formation of some CO that poisoned the Pt electrode [8].

In situ diffuse reflectance FTIR spectra of a Pt/C catalyst under a CO_2/H_2 10/1 mixture under atmospheric conditions revealed the presence of a broad peak Pt-carbonyl, which was suggested to be able to modify the sample activity for the hydrogenation of halonitroaromatics [19]. Arunajatesan et al. reported the formation of carbonyl species over a Pd/alumina under different conditions ($P = 138$ bar; $T = 342$ K; molar $CO_2/H_2 = 19$) [20]. Based on the presence of water peaks at reaction conditions, these authors proposed that the reverse water–gas shift reaction is the most plausible mechanism for CO formation.

The use of different metals, supports or substrates may allow overcoming the formation of carbonyls and/or catalyst poisoning under CO_2-containing feeds. Recently, Fujita et al. investigated the hydrogenation of phenol with H_2 under high-pressure CO_2 by in situ IR spectroscopy [21]. The formation of Rh-carbonyl species was observed over Rh–Al_2O_3 and Rh/C. The nature and intensity of the carbonyl bands were quite different on each sample and only the alumina-based material showed a complete deactivation.

It must be stressed that beneficial effects due to CO_2 reactivity have also been reported. Wang and co-workers have reported that CO_2 used as a gas diluent during the dehydrogenation of ethyl benzene to styrene also acted as a promoter for the reaction [22]. These authors proposed that ethylbenzene dehydrogenation was coupled with the RWGS (Eq. (1)); hence, the hydrogen formed was effectively being scavenged by the CO_2. Note that this beneficial coupling was observed at a high temperature, i.e. 550 °C, over non-precious transition metals supported on alumina.

Arai and co-workers reported that both conversion and selectivity increased during the hydrogenation of unsaturated aldehydes to unsaturated alcohols over a 1 wt.% Pt/Al_2O_3 at 50 °C in $scCO_2$ [23]. The improvement in activity was suggested to arise from (i) the change of the dielectric constant of the reaction medium, (ii) the increased solubility of reagents and/or (iii) increased mass transport coefficient, although no evidence was provided. The possible formation of CO was not mentioned. Zhao et al. have used $scCO_2$ medium to enhance selective hydrogenation of nitro aromatics over Pt/C [24,25]. These authors reported no deactivation and similar conversions as those measured in ethanol were obtained. The reaction in $scCO_2$ was found to be structure insensitive, while the opposite was true in the case of using the ethanol solvent. Again, no mention of a possible role of carbon monoxide on the activity of the sample was mentioned.

Arai and co-workers [26] showed that strong molecular interactions were taking place between organic substrates and CO_2, particularly at high CO_2 pressures. It is possible that such interactions could be one of the factors affecting the catalyst activity (rate and/or selectivity) during the conversion of the substrate in the presence of CO_2.

While the increased reagent solubility and transfer coefficient (via overcoming of the liquid–gas interface) [27] are likely contributors to improved catalytic properties when working in $scCO_2$, the evidence provided by many authors [15–17,19,21] also suggests that selective site poisoning could be, at least in part, responsible for the improved performance of metal catalysts when using $scCO_2$ and H_2. There seems actually to be some controversy on whether CO formation can be effective and induce poisoning for hydrogenation reactions carried out in the presence of CO_2, as recently discussed by Roberts and co-workers [18].

To better assess the possible role of the RWGS (Eq. (1)) in hydrogenation reactions carried out in the presence of CO_2, we report here an investigation of the hydrogenation of toluene over a Pt/Al_2O_3 catalyst using a simulated biogas, i.e. a $H_2 + CO_2$ mixture. Our primary aim was to determine whether CO poisoning could occur on Pt-based catalysts used at very low temperature (i.e. 75 °C) and atmospheric pressure for a gas–solid system. This set of conditions would be of interest for any commercial hydrogenation reaction using biogas. Toluene was selected as a test molecule, the hydrogenation of which is often considered as non-structure sensitive [28,29].

Preliminary reactivity tests conducted using a classical stainless steel tubular reactor showed that a strong deactivation occurred in the presence of CO_2. An in-depth operando diffuse reflectance FTIR spectroscopy (DRIFTS) study was then carried out to attempt to relate the deactivation to observable surface species. Discriminating between surface species is important because toluene hydrogenation has been shown to proceed also on the support in the case of many oxide-supported Pt catalysts, supposedly due to hydrogen spill-over onto the support and hydrogenation of toluene on the support sites [30]. It appeared that the deactivation observed in our case could be quantitatively linked only to the formation of Pt-carbonyl species.

2. Experimental

2.1. Catalyst preparation

The Pt/Al_2O_3 catalyst was prepared using γ-alumina particles impregnated by a platinum acetyl-acetonate solution. The size of the alumina particles (from Sasol Chemie) was in the range 150–250 μm with a specific surface area of 155 m^2/g. One hundred and fifty grams of alumina powder was mixed with 200 ml toluene and 3.13 g of platinum acetyl-acetonate. The mixture was stirred for 3 h at 60 °C. The solvent was then removed by evaporation at 80 °C under reduced pressure. The resulting powder was then dried at 120 °C for one night. This catalyst was then calcined in ambient air at 500 °C for 4 h using a temperature ramp of 3 °C/min. After preparation, the platinum content on the catalyst was about 0.88 wt.% and the Pt dispersion, measured by H_2 chemisorption (see sample pre-treatment details in the Supplementary material), was about 54%.

2.2. Catalytic tests in a tubular stainless steel reactor

The standard procedure for catalyst activation consisted in an in situ reduction at 350 °C (heating ramp of 3 °C/min) for 4 h under hydrogen flow of 80 ml/min (STP). The dinitrogen, carbon dioxide and dihydrogen used were provided by Air Liquide under the purity category of Alpha Gaz 1, specifically containing $H_2O < 3$ ppm, $O_2 < 2$ ppm and CnHm < 0.5 ppm. The toluene was obtained from Sigma Aldrich with a purity above 99.5%.

The feed composition consisted of a mixture made of 10% toluene + 45% (N_2 or CO_2) in H_2. The catalytic experiments were conducted in a packed-bed stainless steel tube reactor (10 cm in height, 6 mm internal diameter). The 10-cm-long reactor was inserted in a 20-cm-long copper shell, the thickness of which was 5 cm. The copper shell was then wrapped with heating jackets. The absence of any temperature gradient within the reactor length was confirmed by measurement using a thermocouple. The reactor was loaded with 2 g of catalyst and the resulting bed was ca. 5 cm in height. The bed was held between two 5 mm layers of quartz particles, those being located between two layers of SiC.

The gas analysis was carried out using a HP Series II 5890 Gas chromatograph fitted with a thermal conductivity (TCD) detector. Two columns PoraBond Q (length = 25 m, diameter = 0.32 mm and thickness = 5 μm) and Molsieve 5A (length = 10 m, diameter = 0.32 mm and thickness = 10 μm) provided by Varian were employed. The gas samples were injected online with helium as carrier gas. The oven temperature was maintained at 50 °C for 2 min to allow peak separation. After each injection, the column temperature was increased to 200 °C to get rid of any water and carbon dioxide adsorbed on the molecular sieve.

2.3. Operando diffuse reflectance FTIR analysis

A high-pressure high-temperature diffuse reflectance reaction cell from Spectra-Tech was used. The cell was modified, mostly as described elsewhere [31], to eliminate bed by-pass. The only difference with the modification described in reference [31] is that a quartz wool plug was used in place of a metallic mesh to hold the sample. This was done to limit toluene hydrogenation over the metallic components of the reaction cell (*vide infra*). The modified cell yielded a full conversion of CO in the presence of O_2 after the reaction light-off over the Pt/Al_2O_3 catalyst, showing that no by-pass occurred (Fig. S1, Supplementary material). No CO oxidation activity was recorded over a cell loaded with SiC.

The DRIFTS assembly was fitted in a Nicolet Magna 550 FTIR spectrometer, and a MCT detector cooled with liquid nitrogen was used. Gases (i.e. high purity Ar, O_2, CO_2 and H_2 from Air Liquide) were fed through low volume-heated stainless steel lines to the cell. Toluene was introduced via a saturator kept at 25 °C. The feed composition was different from that used in the kinetic setup and consisted of 1.6% toluene + 40% H_2 + 2 or 40% CO_2 (if present) in Ar. A low partial pressure of toluene was used here to prevent condensation on the DRIFTS cells walls, which were held at around room temperature. The tests were made at atmospheric pressure and at a total flow rate of 25 ml/min. The DRIFTS data are reported as $\log(1/R)$, where R is the sample reflectance. The pseudo-absorbance $\log(1/R)$ gives a better linear representation of the band intensity against sample surface coverage than that given by the Kubelka–Munk function for strongly absorbing media such as those based on alumina [32].The contribution of gas-phase toluene and cyclohexane was subtracted from the surface DRIFTS signal (*vide infra*).

The reaction cell crucible was filled first with a layer of SiC and then topped with 19 mg of catalyst powder. The corresponding ratio between catalyst weight and toluene molar flow rate (noted W/F) was about 1.04 $kg_{cat}\ s\ mol^{-1}$. The cell thermocouple was located at the interface between the SiC and catalyst layers. The sample was first oxidized at 350 °C for 15 min under 20% O_2 in Ar before being reduced for 30 min under 40% H_2 in Ar at the same temperature (heating ramp was about 30 °C min^{-1}). The reference backgrounds were collected at 75 °C over the activated sample using 128 scan at a 4 cm^{-1} resolution. A background using a totally reflecting aluminium mirror was also recorded. During the operando analysis, 8, 16 or 32 scans were collected, depending on the time resolution sought.

Toluene and methylcyclohexane gas-phase concentrations were measured after the DRIFTS cell using an IR gas-cell, the optical pathway of which was about 27 cm. Toluene conversion was calculated on the basis of the concentrations of toluene and methylcyclohexane measured, assuming that no other reaction product was formed. This assumption was reasonable since the gas-phase IR spectra in the 3200–2800 cm^{-1} region could be accurately decomposed using the spectra of pure toluene and methylcyclohexane only. Note that no CO gas-phase could ever be observed, although it might have been present at level not detectable with our gas-cell (ca. 200 ppm).

The availability of the IR spectrum of the gas-phase measured at the exit of the DRIFTS cell enabled correcting the DRIFTS spectrum from any gas-phase contribution. A correcting factor of 0.25 was applied, which corresponded to the ratio between the optical path-length in the DRIFTS cell (which depends partly on the catalyst bed properties) and that in the gas-cell. This ratio was determined after the spectrokinetic experiment by flowing pure CO over the catalyst and rationing the area of the gas-phase signal of CO measured in the DRIFTS cell to that obtained in the gas-cell. The effective path-length in the DRIFTS cell (through the void above the bed + multiple reflections in the catalyst bed) was found to be about 6.75 cm. An example of a gas-phase-corrected DRIFTS spectrum and the corresponding original spectrum are given in Fig. S2.

The DRIFTS cell loaded with inert SiC presented a non-negligible activity for toluene hydrogenation to methylcyclohexane (about 4% conversion at 75 °C in the absence of CO_2 and 3.6% in the presence of CO_2). Most of the exposed naked heating wires that were present in the original cell were covered with a ceramic coating, but with no effect. The observed activity could possibly due to a reaction occurring on remaining exposed heating wires and/or the thermocouple guide. The conversion due to the cell (i.e. 4%) was subtracted from that measured with the catalyst when calculating TOF numbers. Note that the effect of the cell on toluene conversion would certainly depend on the experimental conditions, in particular the total gas flow rate, therefore requiring to measure the cell residual activity under appropriate conditions.

3. Results and discussion

3.1. Kinetic measurements in the tubular stainless steel reactor

The toluene conversions obtained for various W/F over the Pt/Al_2O_3 catalyst at 75 °C and atmospheric pressure in the stainless steel tubular reactor are given in Table 1. The catalyst was active for toluene hydrogenation in the absence of CO_2. The turnover frequency (TOF, Table 1) calculated on the basis of Pt surface atoms (and for conversions <100%) was about $0.11 \pm 0.01\ s^{-1}$. Note that these TOF were the average values from the TOF changing along the catalyst bed in the reactor, because of the integral flow nature of the reactor.

Toluene hydrogenation on Pt is usually reported as a structure-insensitive reaction [28,29], and therefore, the TOF measured here should be similar to those reported in the literature. Rousset et al. have reported that the toluene hydrogenation TOF of a 0.06 wt.% Pt/Al_2O_3 was about 0.12 s^{-1} at 75 °C, using 2.5% toluene in H_2 [33]. Since a zeroth-order in toluene and an order of 0.5 in H_2 were measured [33], the TOF of Rousset et al. extrapolated to our conditions should be around 0.08 s^{-1}. Assuming that the same kinetic orders apply, the TOF values reported by Lin and Vannice [30] for a 0.78 wt.% Pt/Al_2O_3 would roughly correspond to 0.03 s^{-1} translated into our conditions. Our TOF values measured in the tubular stainless steel reactor are therefore of the same order of magnitude as those reported in the literature, the differences noted could possibly be due to the error introduced during the extrapolation or experimental errors associated with the measurements. It must be made clear that the point of our work was not to investigate whether toluene hydrogenation on Pt is truly a structure-insensitive reaction.

No toluene conversion to methylcyclohexane was obtained over the Pt/Al_2O_3 catalyst when carbon dioxide was present (Table 1), indicating that the hydrogenation activity of the sample was strongly inhibited by CO_2. In another experiment (Fig. 1), the conversion was measured following a series of CO_2 pulses into the feed and resulted in a gradual and irreversible deactivation. The reduction of the catalyst using the standard procedure (4 h under H_2 at

Table 1
Catalytic activity in toluene hydrogenation measured in the microkinetic setup at 75 °C and atmospheric pressure over the Pt/Al_2O_3. The last line reports the activity of the some catalyst measured in the DRIFTS cell.

Feed composition (vol.%)				Catalyst weight/ toluene molar flow (kg_{cat} s/mol)	Toluene conversion (%)	TOF (s^{-1})
H_2	N_2	CO_2	Toluene			
45	45	0	10	50	100	0.08 ± 0.01
45	45	0	10	30	74.9	0.10 ± 0.01
45	45	0	10	20	60.2	0.12 ± 0.01
45	0	45	10	50	0	0
40	58.4[a]	0	1.6	1.04	8.6[b]	0.054 ± 0.01

[a] Ar was used in place of N_2.
[b] This value has been corrected for the conversion measured over the cell loaded with SiC (ca. 4%).

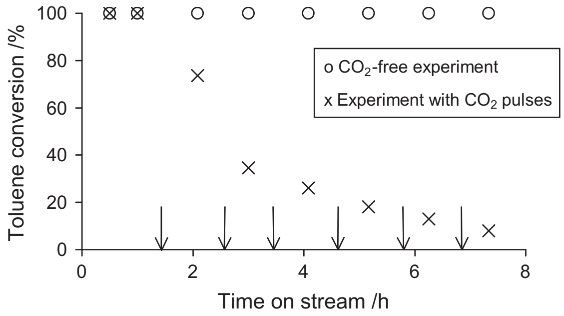

Fig. 1. Conversion of toluene in the reactor used for kinetic studies with (*x*) and with no (○) CO_2 pulses. Feed: 10% toluene + 45% H_2 in N_2. *W*/*F* = 50 kg_{cat} s/mol. *T* = 75 °C. The arrows indicate the various times at which 3.5×10^{-6} moles of CO_2 were injected into the feed.

350 °C) did not allow regaining any activity in the absence of CO_2. However, the Pt/Al_2O_3 treated with air at 300 °C and then reduced using the standard procedure allowed full regeneration (data not shown).

The inhibition of toluene hydrogenation in the presence of CO_2 could be the result of several effects, for instance (i) a simple competitive adsorption between CO_2 and one of the reactants (which should yet be a reversible effect), (ii) the formation of poisonous CO through the RWGS and/or (iii) the formation of poisonous water through CO_2 methanation. The relevance of these various effects will be assessed by the spectrokinetic data collected over the DRIFTS cell described in the following sections.

3.2. Kinetic measurements in the modified DRIFTS cell

Spectroscopic cells are not ideal kinetic reactors, and therefore, it is crucial to check that the reaction rate or TOF measured in these reactors is consistent with that obtained with traditional non-spectroscopic units. Published work reporting agreeing reaction rates between conventional reactors and spectroscopic cells (all spectroscopies being considered) are actually very few [33–37]. A recent review discusses these examples as well as the many pitfalls that the spectroscopic cell experimentalist may face (in particular difficulties with temperature control) while attempting to determine reaction rates in such cells [38].

The modified DRIFTS cell used here presented no bed by-pass, as evidenced by the total CO conversion obtained during CO oxidation above the light-off temperature (Fig. S1, Supplementary material). Unfortunately, the cell itself (simply loaded with inert SiC) presented a non-negligible activity for toluene hydrogenation, which needed to be taken into account when calculating the catalyst TOF (see experimental section).

The initial TOF measured over our Pt/Al_2O_3 catalyst at 75 °C and atmospheric pressure in the DRIFTS cell reactor was $0.054 \pm 0.010\ s^{-1}$ (Table 1). The precision margin was estimated from the various sources of error involved in the TOF calculation, not least the relative error on the conversion measurement estimated at 10%. A TOF corrected value of $0.057\ s^{-1}$ was calculated to allow a comparison with the TOF values obtained with the partial pressures used in the case of the tubular reactor data discussed in the previous section (assuming a 0.5 reaction order for H_2 and zeroth-order in toluene). The corrected value of the TOF measured in the DRIFTS cell (i.e. $0.057 \pm 0.010\ s^{-1}$) appeared to be significantly lower than those obtained in the case of the tubular stainless steel reactor, i.e. $0.11 \pm 0.01\ s^{-1}$ (Table 1).

This discrepancy could be due in part to the fact that about 26% of the Pt sites were still covered by carbonyl species after an insufficiently long reduction in the DRIFTS cell (*vide infra*, the presence of these carbonyls will actually be useful in understanding the surface reactivity of the catalyst). Another possible reason for the discrepancy could be due to a lower effective temperature in the sample zone. Assuming that the apparent activation energy of the reaction was about 50 kJ/mol as reported by Lin and Vannice on similar materials [30], a temperature drop from 75 to 70 °C would lead to a TOF loss of about 22%. It is possible that the temperature of the bed was lower, due to the thermal coupling between the reaction cell walls (kept at room temperature) and the catalyst bed in the presence of large concentrations of H_2, which exhibits a high thermal conductivity. These two possible effects could by themselves alone explain the ca. 50% lower TOF measured in our DRIFTS cell. Despite these shortcomings, the DRIFTS results discussed in the following sections will bring reliable and valuable insights into the effect of CO_2 on the hydrogenation of toluene over this catalyst.

3.3. In situ DRIFTS study of the sample activation

In situ DRIFTS analyses were conducted to monitor the state of the catalyst surface during the sample activation. Physisorbed water (band at 1645 cm^{-1}) and various carbonate/formate/carboxylate species (broad ill-defined bands in the 1700–1200 cm^{-1} region) were observed on the fresh sample (Fig. S3, Supplementary material). The broad band centred around 2070 cm^{-1} was due to the so-called ABC contour associated with combination bands of hydroxyl groups [39], i.e. it was not a carbonyl species.

During oxidation at 350 °C, sharper bands were present in the 1600–1200 cm^{-1} region and no bands could be observed in the carbonyl stretching region (Fig. S3). The intensity of the formate/carbonate bands decreased significantly when H_2 was introduced at 350 °C and a new band was observed at ca. 2020 cm^{-1} (Figs. S3 and 2A), which can be assigned to Pt-carbonyl species adsorbed on Pt-defective site of high index planes or small Pt particles [40–42]. These carbonyls were formed from the reduction of the various surface species above described, directly at the surface or via gas-phase CO_2 [43]. The intensity of the band at 2020 cm^{-1} gradually decreased with increasing time under H_2, while a new low-intensity band appeared at ca. 2090 cm^{-1} (Fig. 2A).

The nature of the 2090 cm^{-1} band is unclear, and tentative assignments are discussed below. On-top Pt–H species exhibit

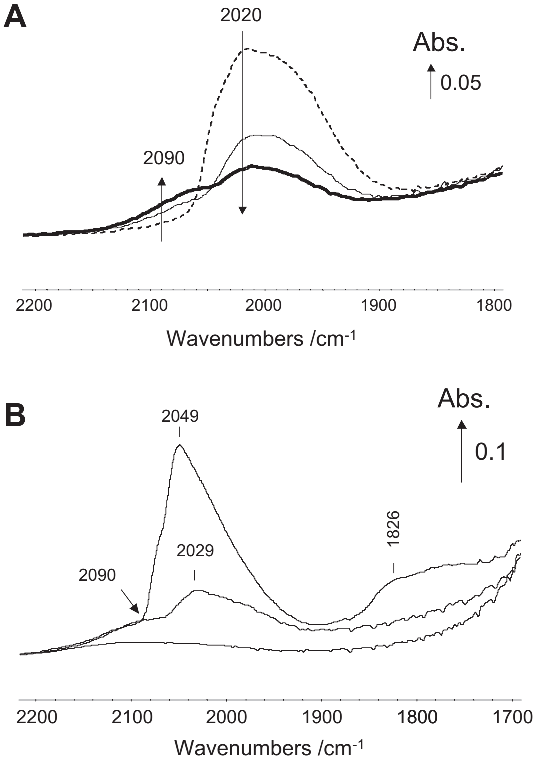

Fig. 2. (A) In situ DRIFTS spectra of the Pt/Al_2O_3 catalyst during the reduction stage at 350 °C under 40% H_2. The spectra were recorded 1 min (dotted line), 15 min (thin solid line) and 30 min (thick solid line) after introducing the H_2 at 350 °C. The spectrum recorded over a mirror was used as background in all cases. (B) In situ DRIFTS spectra of the Pt/Al_2O_3 catalyst after reduction at 350 °C under 40% H_2. The spectra were recorded under H_2 (middle line), at equilibrium condition under 800 ppm of CO (top line) and subsequently under O_2 (bottom line). T = 75 °C. The spectrum recorded over a mirror was used as background in all cases.

weak IR bands at 2120 cm^{-1} and at ca. 2060 cm^{-1}, but these bands are almost impossible to observe when carbonyls are also present [44,45]. Bands at 2090 cm^{-1} are commonly assigned to CO adsorbed on highly coordinated Pt atoms of low index planes. It must be stressed that the dispersion of the Pt was 54% and therefore the average crystallite size is expected to be around 2 nm. The gradual apparition of 2090 cm^{-1} band would, at first, suggest the sintering of some of the small Pt particles to form larger less defective crystals. The occurrence of sintering rationalizes the fact that the carbonyl associated with the defective sites (2020 cm^{-1} band) would be vanishing while others associated with low index planes (2090 cm^{-1} band) would be formed. The former sites typically exhibit much larger CO adsorption enthalpies and are therefore expected to be preferentially covered, when both sites are present. However, the observations described in the following paragraph question this sintering hypothesis.

The sample obtained after H_2 reduction at 350 °C was subsequently exposed to 800 ppm of CO at 75 °C for a few minutes leading to surface saturation with carbonyl species (Fig. 2B). The band at ca. 2020–2029 cm^{-1} grew markedly in intensity, also blue shifting up to 2049 cm^{-1} at saturation. Such blue shift is expected when carbonyl surface concentration increases, because of increased dipole–dipole interactions and a decrease in the average Pt electron back-donation [42]. Bridged carbonyls were also observed below 1900 cm^{-1}. On the contrary, no intensity change was observed at 2090 cm^{-1}, indicating that the corresponding sites were already at saturation before exposure to the 800 ppm of CO. The spectrum obtained under O_2 is also shown, showing that all these bands were removed by oxidation at 75 °C (Fig. 2.B). Incidentally, these data indicate that the proportion of CO adsorption sites that were occupied after reduction with H_2 at 350 °C was approximately 26%. It is unlikely that Pt sites of extended dense planes with high coordination would be fully occupied before most defect sites are covered, even by considering the minor energetic gain that could be associated with island formation. It is therefore unlikely that the growth of the 2090 cm^{-1} band was related to Pt sintering.

In another experiment also at 75 °C, a reduced sample (never exposed to CO) was left under pure Ar after removing the 40% H_2 present. The carbonyl bands showed a minor yet significant red shift upon removing H_2, showing that hydrogen adatoms were present on the Pt particles and interacted with the adsorbed CO (Fig. S4). The fact that the carbonyl IR bands blue shift when H_2 is present can be due to an increased local concentration of carbonyls (e.g. island formation) due to repulsive interactions between CO and H adatoms, as shown for the case of Pt(1 1 1) surfaces by Hoge et al. [46]. The 2090 cm^{-1} signal could thus correspond, somewhat unexpectedly, to small defective particles that were saturated with adsorbed CO, possibly involving multicarbonyl species [47–50]. Strong dipole coupling, neighbouring H adatoms (which are rarely present in most IR studies investigating the nature of Pt-carbonyls) and reduced electron back-donation from the Pt atoms to the carbonyls would all lead to a blue shift of the carbonyl wavenumber. More work would clearly be needed to ascertain this assignment.

Whatever the exact nature of the sites leading to the bands at around 2020 cm^{-1} (shifting to 2049 cm^{-1}) and at 2090 cm^{-1}, our data show that various Pt surface sites were present and that some of those (ca. 26%) were covered with carbonyl following the 30-min reduction in H_2 350 °C. It is likely that using a longer reduction period (e.g. 4 h, as for the kinetic data collected over the tubular reactor) could have led to a full removal of these carbonyls. The presence of these residual carbonyls will yet prove useful in understanding further the adsorption properties of the metal.

3.4. In situ DRIFTS study of toluene hydrogenation

The Pt/Al_2O_3 sample was exposed to toluene and H_2 at 75 °C, following the reduction at 350 °C. New strong bands were observed, in particular in the 3110–2700 cm^{-1} region, corresponding to the stretching vibration of the CH bonds of adsorbed toluene (Fig. 3, middle spectrum). A difference spectrum between the toluene-containing and toluene-free cases is given in Fig. 4 for the sake

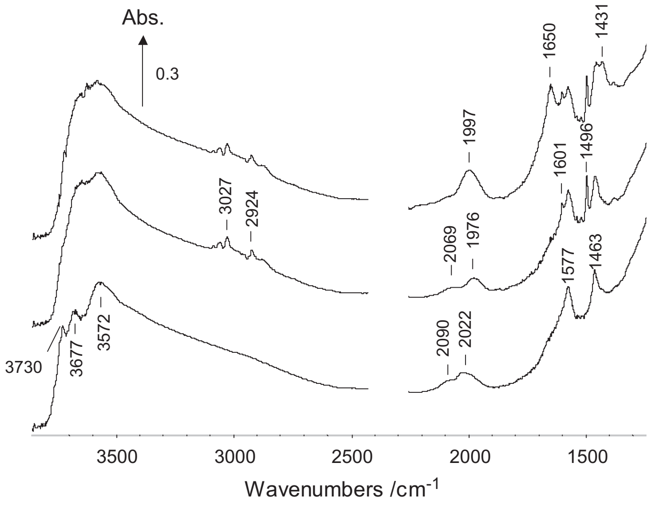

Fig. 3. In situ DRIFTS spectra of the Pt/Al_2O_3 catalyst: after reduction at 350 °C under 40% H_2 (bottom), subsequently exposed to the toluene/H_2 feed (middle), and then 40 s following the addition of 40% CO_2 in the feed (top). T = 75 °C, the spectrum recorded over a mirror was used as background in all cases. The spectra were offset for the sake of clarity. The contribution of gas-phase species was subtracted.

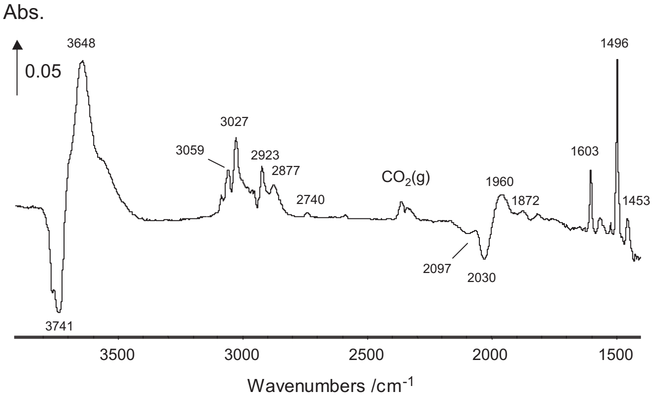

Fig. 4. DRIFTS spectrum of Pt/Alumina after 30 min under H_2/toluene. $T = 75$ °C, the spectrum of the activated sample was recorded at the same temperature under Ar/H_2 and used as background. The contribution of gas-phase species was subtracted. The observed CO_2(g) was ambient CO_2, not in the system.

of clarity. The negative bands at 3741 cm^{-1} indicated that some of the alumina surface hydroxyl groups were in interaction with toluene molecules, resulting in the broad H-bonded hydroxyl band at 3648 cm^{-1} (Fig. 4). Toluene was therefore adsorbed in significant quantities on the support. All the other bands indexed in Fig. 4 (except for those around 2000 cm^{-1}) can be assigned to adsorbed toluene, the spectrum of which is similar – but not identical – to that of the gas-phase molecule [51].

Gas-phase methylcyclohexane [52] exhibits two major bands at 2930 and 2860 cm^{-1}, which overlap with those of toluene, so it is difficult to assess whether the bands of this compound were also present on the spectrum reported in Fig. 4. The adsorption enthalpy of methylcyclohexane on the support but also on Pt is expected to be much lower than that of toluene [53]. By comparison, on Pt(1 1 1), the adsorption enthalpy of benzene is 71 kJ mol^{-1}, while that of cyclohexane is only 27 kJ mol^{-1} [14]. It is therefore expected that methylcyclohexane desorption would be extremely fast once formed and the corresponding steady-state coverage on the catalyst should be negligible.

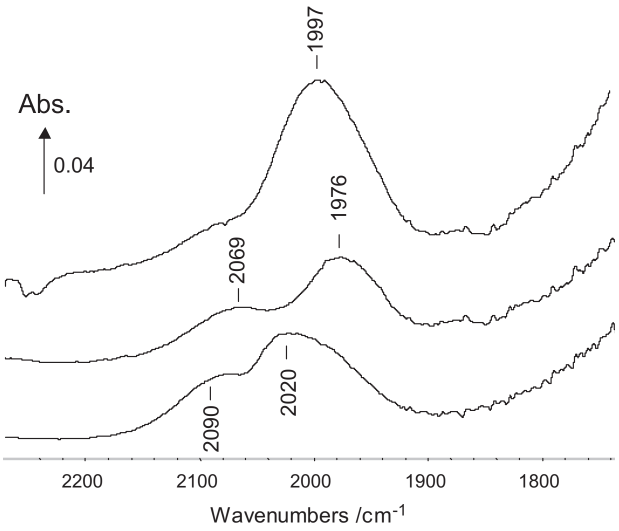

Fig. 5. Magnification of the carbonyl stretching region related to Fig. 3. In situ DRIFTS spectra of the Pt/Al_2O_3 catalyst: after reduction at 350 °C under 40% H_2 (bottom), subsequently exposed to the toluene/H_2 feed (middle), and then 40 s following the addition of 40% CO_2 in the feed (top). $T = 75$ °C, the spectrum recorded over a mirror was used as background in all cases.

The carbonyl bands were still present following toluene adsorption, although those were modified (mostly shifted) when compared to the case of the sample under H_2 after reduction (Figs. 3 and 4). A zoom-in of the carbonyl region is also given in Fig. 5 for the sake of clarity. The modification of the Pt-bound carbonyl signal clearly indicates that the hydrocarbon adsorbed also on the Pt. The two main carbonyl bands shifted towards lower wavenumber upon toluene introduction. The shifts were reversible when toluene was removed, although the intensity of the 2020 cm^{-1} band was significantly decreased (data not shown). This shows that toluene competed with CO for adsorption on the metal, particularly for the sites associated with the carbonyl band at 2020 cm^{-1}. The carbonyl red shift observed in the presence of toluene was most likely due to an increased back-donation of Pt electronic density into the π^* anti-bonding orbital of CO, due to an increased electronic density of the Pt particles following the adsorption of the electron-rich toluene.

3.5. Operando DRIFTS study of the effect of CO_2

The effects of the addition of CO_2 into the toluene/H_2 feed on the catalyst surface were studied by operando DRIFTS, while the toluene conversion to methylcyclohexane was monitored using the FTIR gas-cell located at the DRIFTS cell exit. The evolution of the conversion of toluene is shown in Fig. 6 over various periods with different feed compositions.

An apparent slow deactivation was first noted under the CO_2-free feed, that is for reaction times $t < 0$ s. The origin of this deactivation is unclear. A minor increase (around noise level) in the DRIFTS carbonyl signal suggests that this slow deactivation could be due to the incomplete reduction of the sample (e.g. alumina-supported carbonates still being reduced) or traces of CO_2 or CO contaminant in the system. The deactivation actually slowed down on a later reaction test ($1800\ s < t < 7300\ s$), supporting the view that the cause for the deactivation under CO_2-free conditions was transient in nature. The subsequent data will suggest that any CO contamination level was well below 3 ppm (*vide infra*).

The toluene conversion dropped dramatically as soon as 40% CO_2 was added to the feed at $t = 0$ s, reaching the residual level of activity of the cell after about 1300 s. The DRIFTS spectrum exhibited marked changes already 40 s after the introduction of CO_2 (Figs. 3 and 5). New large bands appeared around 1650 and 1431 cm^{-1}, which could be indicative of the presence of water, carbonate and/or hydrogenocarbonate species. The carbonyl band signal also increased, with the most prominent band absorbing

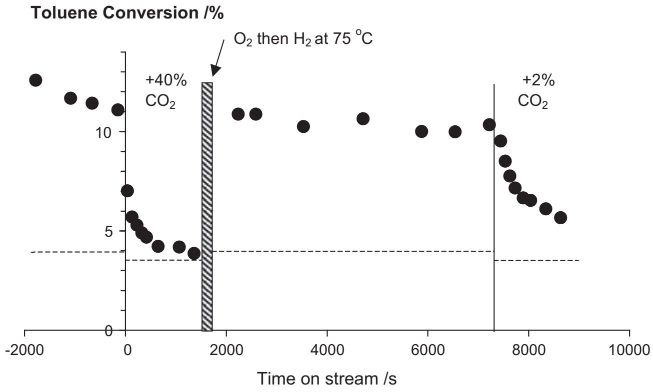

Fig. 6. Toluene conversion over the Pt/Al_2O_3. The concentration of added CO_2 is indicated on the plot for the periods during which this molecule was added to the feed. The conversion due to the DRIFTS cell reactor filled only with SiC is indicated by the dotted lines. Feed: 1.6% toluene + 40% H_2 in Ar. Total pressure = 1 bar, $W/F = 1.04\ kg_{cat}\ s/mol$.

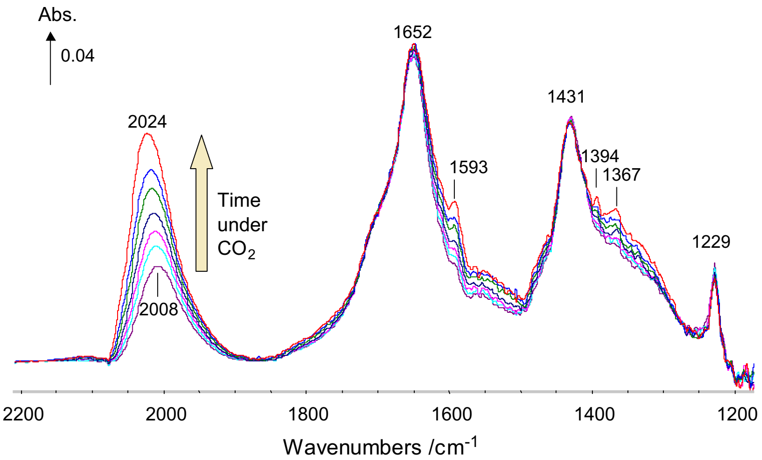

Fig. 7. Operando DRIFTS spectra of the Pt/Al_2O_3 under a toluene/H_2 feed for various times on stream with additional 40% CO_2: 81, 176, 273, 470, 847, 1244 and 3645 s. T = 75 °C, the spectrum of the sample recorded at the same temperature under toluene/H_2 was used as background.

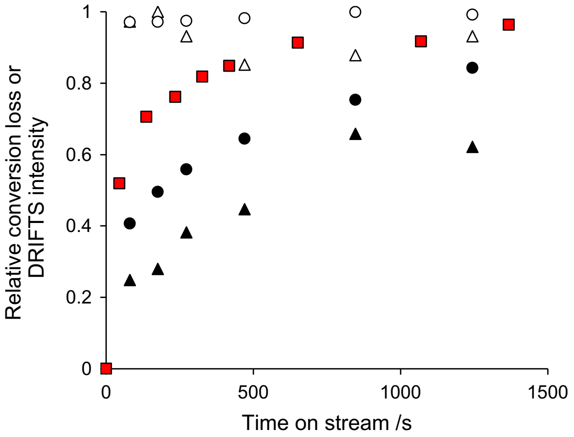

Fig. 8. Correlation of the relative loss of toluene conversion (🟥) with the relative increase in intensity of the species seen by DRIFTS over the Pt/Al_2O_3 following the introduction of 40% CO_2 in the toluene/H_2 feed: carbonyl (●), formate (▲), hydrogenocarbonates (△) and all the bands in the region 1800–1550 cm^{-1} (○).

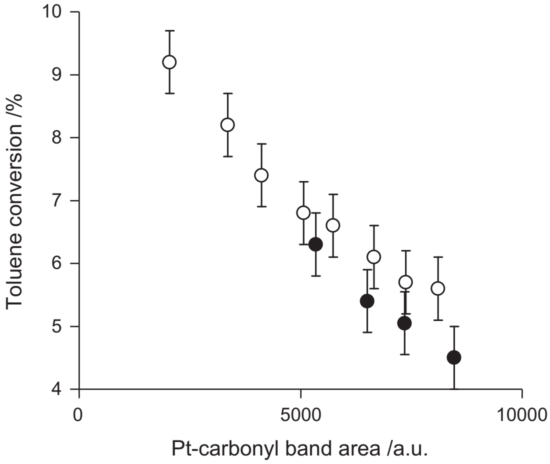

Fig. 10. Correlation between the toluene conversion and the DRIFTS band area of Pt-carbonyl species formed under 2% (○) and 40% (●) CO_2 in the toluene/H_2 feed.

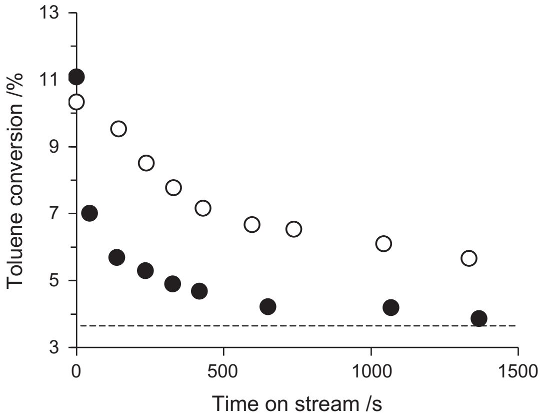

Fig. 9. Effect of the CO_2 concentration on the toluene conversion over the Pt/Al_2O_3. The conversion due to the DRIFTS cell reactor filled only with SiC is indicated by the dotted line. Feed: 1.6% toluene + 40% H_2 + 2 (○) or 40 (●) % CO_2 in Ar. Total pressure = 1 bar, W/F = 1.04 kg_{cat} s/mol.

now at 1997 cm^{-1} (Fig. 5). Interestingly, the surface concentration of toluene did not appear to change, as shown by the constant area of the band at 3030 cm^{-1} (Fig. 3). Since most of the toluene DRIFTS signal comes from species adsorbed on the alumina, this stresses that there was essentially no competitive adsorption between toluene and CO_2-derived species formed on the support under our experimental conditions.

Difference spectra were calculated for the CO_2-containing data by subtracting the spectrum collected just before the introduction of CO_2 (this is equivalent to taking the sample under toluene/H_2 as background). This allowed observing more easily the modifications occurring upon CO_2 introduction (Fig. 7). The structure of the new growing carbonyl band appeared more clearly as essentially a single peak, which was growing with time and shifting towards higher wavenumbers from 2008 to 2024 cm^{-1} as the concentration of Pt–CO increased. The blue shifting of this band was probably related to the increasing surface concentration of carbonyl through (i) the decrease in the average electronic density of Pt available for back-donation into the carbonyl π^* anti-bonding orbital, (ii) the increase in CO(ads) dipole–dipole interactions [42,54] and (iii) the likely displacement of some or all the (electron-rich) toluene adsorbed on the metal.

The difference spectra (Fig. 7) made more obvious the 1229 cm^{-1} band, which is assigned to the bending mode of the hydroxyl group of the hydrogenocarbonate species (the other corresponding bands being at 1652 and 1431 cm^{-1}) [55]. The hydrogenocarbonate species therefore appeared to be the main surface species formed under CO_2 and was probably formed from the reaction of CO_2 and an alumina surface hydroxyl group [56]. Additional bands with a positive growth were observed at 1589, 1394 and 1369 cm^{-1}, which corresponds to formate species, probably formed by the reaction of CO with alumina surface hydroxyl groups [56]. It is likely that there were also other carbonate-type species and water present, the signal of which would overlap with the major bands already discussed.

The possible link between the decrease in the toluene conversion and the various surface species observed by DRIFTS was assessed by plotting the relative variation of the area of the corresponding signals (Fig. 8). The species correlating best with the loss of conversion appeared to be the newly formed carbonyl, followed by the formates. The hydrogenocarbonate signal was not correlated with the decrease in the reaction product signal and can be discarded as the main origin of the deactivation. It is interesting to note that full deactivation appeared to be reached before the saturation of the Pt sites with carbonyl (Fig. 8). This could be rationalized by the fact that an ensemble of sites is actually needed to obtain toluene conversion, e.g. requiring adsorption sites for both H_2 and toluene. The number of available sites in a domain has been suggested to be crucial in determining selective hydrogenation pathways over Pd-based catalysts [57].

Similar conclusions on the deactivating role of CO_2 were obtained in the case of exposing the sample to a much lower concentration of CO_2, i.e. 2%. The corresponding toluene conversion data are reported in Fig. 6, for $t > 7300$ s. The conversion decay appeared to be slower when compared to the case of the 40% CO_2, as confirmed by the data replotted in Fig. 9. The growth of the carbonyl and hydrogenocarbonate species was also slower in the case of the feed with the least CO_2 (Figs. S5 and S6). It must be stressed that the formate signal was negligible in the case of the deactivation occurring under the feed containing the 2% CO_2, stressing that formates were not the origin of the loss of activity.

Therefore, the carbonyls formed at ca. 2000 cm^{-1} were the only observable surface species that could be linked to the decreasing activity in toluene hydrogenation. The relation between catalyst activity and the area of the DRIFTS band of the carbonyls is plotted in Fig. 10 for both CO_2 concentrations. It is striking that there was an unequivocal relation between the carbonyl band intensity and the level of conversion remaining, independently of the CO_2 partial pressure. These data therefore prove that the poisoning of Pt by strongly bound carbonyl was the main reason for the loss of toluene hydrogenation activity in the presence of CO_2.

It must be noted that the catalyst could be fully regenerated in situ at 75 °C by passing an O_2 feed for a few seconds (Fig. 6). This is clearly not sufficient for improving the applicability of the present material and clearly other formulations will have to be developed to provide stable conversions.

It is not clear whether any gas-phase CO was actually produced under our reaction conditions. It is possible that a minute amount of CO_2 would decompose to CO(ads) and O(ads) over the sample, with no CO ever leaving the catalyst surface (the O can be scavenged by hydrogen to form water). To investigate this matter, the rate of the reverse water–gas shift (RWGS) reaction was measured over our DRIFTS cell. No CO could be observed below 200 °C (our CO(g) detection limit was about 200 ppm). Significant concentration of CO and methane was obtained above 250 °C (Fig. S7) and an arrhenius-type plot was constructed using these data points (Fig. S8) to estimate back the theoretical level of CO that could be formed at 75 °C, if the linear relationship were to hold. A level of ca. 3 ppm of CO could thus be expected from a RWGS feed with concentrations of H_2 and CO_2 of 50% and 2%, respectively, which were similar to that used the toluene hydrogenation experiment described in Fig. 6 for $t > 7300$ s.

The true level of CO(g) is likely to be lower, because CO desorption might become insignificant at low temperatures. In conclusion, the concentration level of CO that was possibly present and deactivated the catalyst under the 2% CO_2-containing feed was likely to be less than 3 ppm. This also shows that the level of CO impurity in our system was far less than 3 ppm of CO, since the deactivation rate measured in the absence of CO_2 was much slower than that observed under 2% CO_2 (Fig. 6, $t > 2000$ s).

3.6. Discussion

Our Pt/Al_2O_3 catalyst was active for the hydrogenation of toluene at 75 °C. It is interesting to note that our pre-reduction procedure led to the formation of Pt-carbonyl species (Figs. 2, 3 and 5), derived from the reduction of the carbonate-type species initially present on the sample (Fig. S2). The carbonyl band was broad and resulted from the overlap of several contributions spanning from 2100 to 1900 cm^{-1}.

This stresses that different reduction temperatures, duration and gas flow rate could lead to different residual coverage of Pt with CO and potentially different extent of Pt poisoning. This observation may explain some of the discrepancies reported in the literature regarding the hydrogenation activity patterns of aromatics over metals [58]. The temperature at which the hydrogenation is conducted used may also lead to different levels of CO removal from the Pt, hence complicating the determination of accurate TOF values.

Operando FTIR work by Ferri et al. carried out in supercritical CO_2 in the presence of H_2 over a model Pt/Al_2O_3 catalyst [59] showed that the presence of large concentration of carbonates on the support surface resulted in the formation of atypical carbonyl species that could not be formed by simple exposure to CO. These unusual carbonyl exhibited bands at ca. 1965 and 1756 cm^{-1} and were assigned to linear and bridged carbonyl adsorbed at Pt-alumina interfacial sites. The band observed here at 1976 cm^{-1} (Figs. 3 and 5) in the presence of toluene and hydrogen could possibly be related to the 1965 cm^{-1} band observed by Ferri et al. [59] on their catalyst. However, upon exposure to CO_2 (Fig. 5) or even CO (Fig. 2), this carbonyl band appeared to shift from ca. 1976 up to 2049 cm^{-1} at saturation. It is therefore reasonable in our case to assign this band to Pt sites that are not interfacial with alumina.

Our data clearly showed that H_2 and toluene adsorbed on some Pt sites in the absence of CO_2, because of the shift that these species produced on the residual carbonyl signal (Fig. S4 and Figs. 4 and 5). We have yet no indication whether the poisoning by carbonyl inhibited the adsorption of toluene or H_2 or both. While CO is a well-known poison of Pt sites needed for H_2 chemisorption in the case of the Pt-based catalysts used in H_2-fuel cells, H_2 can yet compete better for adsorption with CO whenever the concentration of the latter is very low [60], as it is the case for our data ([CO] expected to be lower than 3 ppm in the case of the 2% CO_2-containing feed). It is therefore reasonable to suggest that H_2 activation was not significantly hindered in the present case and that the loss of activity was solely due to the inhibition of toluene adsorption on the metal. In support to this view, Rioux et al. [61] showed that CO was in competition for adsorption with ethylene and not H_2 in the case of the CO-modified ethylene hydrogenation over Pt nanoparticles. More work would yet be required to unambiguously confirm that H_2 adsorption was not hindered in our case.

Our Pt-alumina would clearly not be of any interest for the hydrogenation of many aromatic hydrocarbons using a $H_2 + CO_2$ mixtures. Other catalytic formulations could surely lead to improved stability against CO poisoning, either because CO_2 dissociation would be hindered under relevant experimental conditions or the sample would not be poisoned by CO. Metals such as Ru and Ni supported on alumina did not allow observing any carbonyl species suggesting that these catalysts may be better suited than Pt-based catalysts for hydrogenation in supercritical CO_2 [20]. Also, rhodium supported on carbon support was shown to be less encline to CO poisoning than an alumina-supported Rh, as showed by Fujita et al. [21].

4. Conclusions

The present contribution underlines the benefits of using in situ and operando DRIFTS spectroscopy in investigating the mechanistic features of toluene hydrogenation over a Pt-alumina catalyst. The following main conclusions can be drawn:

1. Some Pt sites were permanently covered with carbonyls derived from carbonate-type species decomposition during sample reductive activation. The fraction of permanently CO-poisoned sites may vary depending on sample pre-treatment and operating conditions, which may affect significantly the determination of accurate TOF values.
2. Toluene adsorbed both on the metal and on the alumina under our experimental conditions.
3. The utilization of a mixture of H_2 and CO_2 for the hydrogenation of toluene at 75 °C resulted in the formation of additional Pt-carbonyl species that strongly poisoned the catalytic activity of our Pt/Al_2O_3. An unequivocal relation was obtained between the level of toluene conversion and the Pt-carbonyl band intensity.
4. The formation of many surface species on the alumina (e.g. carbonate, hydrogenocarbonate, formate) was shown not to be related to the sample deactivation under our experimental conditions.

Acknowledgment

We are thankful to Government of Pakistan (Higher Education Commission) for supporting this research work through doctoral grant to Aqeel Ahmad TAIMOOR.

Appendix A. Supplementary data

Supplementary data associated with this article can be found, in the online version, at doi:10.1016/j.jcat.2010.12.002.

References

[1] Debabrata Das, T. Nejat Veziroglu, Int. J. Hyd. Energy 26 (2001) 13.
[2] J. Wang, Wei Wan, Int. J. Hyd. Energy 34 (2009) 799.
[3] M. Huang, S. Kaliaguine, S. Suppiah, Appl. Surf. Sci. 90 (1995) 393.
[4] L. Chen, B. Chen, C. Zhou, J. Wu, R.C. Forrey, H. Cheng, J. Phys. Chem. C 112 (2008) 13937.
[5] A. Goguet, D. Tibiletti, F.C. Meunier, J.P. Breen, R. Burch, J. Phys. Chem. B 108 (2004) 20240.
[6] G.W. Roberts, P. Chin, X. Sun, J.J. Spivey, Appl. Catal. B: Environ. 46 (2003) 601.
[7] R.A. Dagle, A. Platon, D.R. Palo, A.K. Datye, J.M. Vohs, Y. Wang, Appl. Catal. A: Gen. 342 (2008) 63.
[8] T. Gu, W.-K. Lee, J.W. Van Zee, Appl. Catal. B: Gen. 56 (2005) 43.
[9] G. Papoian, J.K. Noskov, R.J. Hoffmann, J. Am. Chem. Soc. 122 (2000) 4129.
[10] K. Chrismann, Surf. Sci. Rep. 9 (1988) 1.
[11] D. Godbey, G.A. Somorjai, Surf. Sci. 204 (1988) 301.
[12] M.T.M. Koper, T.E. Shubina, R.A. van Santen, J. Phys. Chem. B 106 (2002) 686.
[13] S.E. Mason, I. Grinberg, A.M. Rappe, J. Phys. Chem. C 112 (2008) 1963.
[14] M. Saeys, M.-F. Reyniers, J.W. Thybaut, M. Neurock, G.B. Marin, J. Catal. 236 (2005) 129.
[15] M. Burgener, D. Ferri, J.-D. Grunwaldt, T. Mallat, A. Baiker, J. Phys. Chem. B 109 (2005) 16794.
[16] B. Minder, T. Mallat, K.H. Pickel, K. Steiner, A. Baiker, Catal. Lett. 34 (1995) 1.
[17] R. Wandeler, N. Künzle, M.S. Schneider, T. Mallat, A. Baiker, Chem. Commun. 7 (2001) 673.
[18] Dawei Xu, R.G. Carbonell, D.J. Kiserow, G.W. Roberts, Ind. Eng. Chem. Res. 44 (2005) 6164.
[19] S. Ichikawa, M. Tada, Y. Iwasawa, T. Ikariya, Chem. Commun. 7 (2005) 924.
[20] V. Arunajatesan, B. Subramaniam, K.W. Hutchenson, F.E. Herkes, Chem. Eng. Sci. 62 (2007) 5062.
[21] S.-I. Fujita, T. Yamada, Y. Akiyama, H. Cheng, F. Zhao, M. Arai, J. Supercrit. Fluids 54 (2010) 190.
[22] A. Sun, Z. Qin, S. Chen, J. Wang, J. Mol. Catal. A: Chem. 210 (2004) 189.
[23] B.M. Bhanage, Y. Ikushima, M. Shirai, M. Arai, Catal. Lett. 62 (1999) 175.
[24] F. Zhao, S.-I. Fujita, J. Sun, Y. Ikushima, M. Arai, Catal. Today 98 (2004) 523.
[25] F. Zhao, Y. Ikushima, M. Arai, J. Catal. 224 (2004) 479.
[26] X. Meng, H. Cheng, Y. Akiyama, Y. Hao, W. Qiao, Y. Yu, F. Zhao, S.-I. Fujita, M. Arai, J. Catal. 264 (2009) 1.
[27] H.-S. Phiong, F.P. Lucien, A.A. Adesina, J. Sup. Fluids 25 (2003) 155.
[28] M. Boudart, Chem. Rev. 95 (1995) 661.
[29] D.S. Cunha, G.M. Cruz, Appl. Catal. A: Gen. 236 (2002) 55.
[30] S.D. Lin, M.A. Vannice, J. Catal. 143 (1991) 554.
[31] F.C. Meunier, A. Goguet, S. Shekhtman, D. Rooney, H. Daly, Appl. Catal. A 340 (2008) 196.
[32] J. Sirita, S. Phanichphant, F.C. Meunier, Anal. Chem. 79 (2007) 3912.
[33] B.S. Clausen, G. Steffensen, B. Fabius, J. Villadsen, R. Feidenhans, H. Topsøe, J. Catal. 132 (1991) 524.
[34] M.A. Bañares, S.J. Khatib, Catal. Today 96 (2004) 251.
[35] F.C. Meunier, D. Reid, A. Goguet, S. Shekhtman, C. Hardacre, R. Burch, W. Deng, M. Flytzani-Stephanopoulos, J. Catal. 247 (2007) 277.
[36] S.R. Bare, N. Yang, S.D. Kelly, G.E. Mickelson, F.S. Modica, Catal. Today 126 (2007) 18.
[37] S. Chansai, R. Burch, C. Hardacre, J. Breen, F.C. Meunier, J. Catal. 276 (2010) 49.
[38] F.C. Meunier, Chem. Soc. Rev. 39 (2010) 4602.
[39] G. Busca, Phys. Chem. Chem. Phys. 1 (1999) 723.
[40] C. Elmasides, X.E. Verykios, J. Catal. 203 (2001) 477.
[41] J. Yoshinobu, M. Kawai, Surf. Sci. 363 (1996) 105.
[42] P. Hollins, Surf. Sci. Rep. 16 (1992) 51.
[43] T. Lear, N.G. Hamilton, D. Lennon, Catal. Today 126 (2007) 219.
[44] T. Szilagyi, J. Catal. 121 (1990) 223.
[45] L.T. Dixon, R. Barth, J.W. Gryder, J. Catal. 37 (1975) 368.
[46] D. Hoge, M. Tueshaus, A.M. Bradshaw, Surf. Sci. 207 (1988) L935.
[47] J. Novakova, J. Mol. Catal. A: Chem. 169 (2001) 247.
[48] K. Chakarova, K. Hadjiivanov, G. Atanasova, K. Tenchev, J. Mol. Catal. A: Chem. 264 (2007) 270.
[49] G.H. Yokomizo, C. Louis, A.T. Bell, J. Catal. 120 (1989) 1.
[50] S.Y. Chin, C.T. Williams, M.D. Amiridis, J. Phys. Chem. B 110 (2006) 871.
[51] <http://webbook.nist.gov/cgi/cbook.cgi?ID=C108883&Units=SI&Type=IR-SPEC&Index=1#IR-SPEC>.
[52] <http://webbook.nist.gov/cgi/cbook.cgi?ID=C108872&Units=SI&Type=IR-SPEC&Index=1#IR-SPEC>.
[53] R.I. Slioor, J.M. Kanervo, A.O.I. Krause, Catal. Lett. 121 (2008) 24.
[54] D. Tibiletti, A. Goguet, D. Reid, F.C. Meunier, R. Burch, Catal. Today 113 (2006) 94.
[55] C. Binet, A. Jadi, J.C. Lavalley, J. Chim. Phys. Phys. Chim. Biol. 86 (1989) 471.
[56] J.C. Lavalley, Catal. Today 27 (1996) 377.
[57] N. Lopez, B. Bridier, J. Pérez-Ramírez, J. Phys. Chem. C 112 (2008) 9346.
[58] M.A. Keane, P.M. Patterson, Ind. Eng. Chem. Res. 38 (1999) 1295.
[59] D. Ferri, T. Burgi, A. Baiker, Phys. Chem. Chem. Phys. 4 (2002) 2667.
[60] J.C. Davies, G. Tsotridis, M. Varlam, S. Valkiers, M. Berglund, P. Taylor, Int. J. Mass Spec. 291 (2010) 152.
[61] R.M. Rioux, R. Komor, H. Song, J.D. Hoefelmeyer, M. Grass, K. Niesz, P. Yang, G.A. Somorjai, J. Catal. 254 (2008) 1.